Invited Paper

The new IR and THz FEL Facility at the Fritz Haber Institute in Berlin

Wieland Schöllkopf[a], Sandy Gewinner[a], Heinz Junkes[a], Alexander Paarmann[a], Gert von Helden[a], Hans Bluem[b], Alan M.M. Todd[b]

[a]Fritz-Haber-Institut der Max-Planck-Gesellschaft, Faradayweg 4-6, 14195 Berlin, Germany;
[b]Advanced Energy Systems, Inc., 27 Industrial Blvd., Medford, NY 11763, USA

ABSTRACT

A mid-infrared oscillator FEL has been commissioned at the Fritz Haber Institute. The accelerator consists of a thermionic gridded gun, a subharmonic buncher, and two S-band standing-wave copper structures. It provides a final electron energy adjustable from 15 to 50 MeV, low longitudinal (< 50 keV ps) and transverse emittance ($< 20\,\pi$ mm mrad), at more than 200 pC bunch charge with a micro-pulse repetition rate of 1 GHz and a macro-pulse length of up to 15 μs. Pulsed radiation with up to 100 mJ macro-pulse energy at about 0.5% FWHM bandwidth is routinely produced in the wavelength range from 4 to 48 μm. A characterization of the FEL performance in terms of pulse energy, bandwidth, and micro-pulse shape of the IR radiation is given. In addition, selected user results are presented. These include, for instance, spectroscopy of bio-molecules (peptides and small proteins) either conformer selected by ion mobility spectrometry or embedded in superfluid helium nano-droplets at 0.4 K, as well as vibrational spectroscopy of mass-selected metal-oxide clusters and protonated water clusters in the gas phase.

Keywords: infrared FEL, oscillator FEL, vibrational spectroscopy, action spectroscopy, spectroscopy of bio-molecules

1. INTRODUCTION

At the Fritz Haber Institute (FHI) of the Max Planck Society in Berlin, Germany, an infrared free-electron laser (IR FEL) facility has been in operation for about one and a half years. The FEL provides powerful, pulsed laser radiation at any wavelength continuously tunable from about 4 to 50 μm covering the mid-infrared (MIR) wavelength range. Installation of the FEL started in mid 2011. First lasing was achieved in 2012.[1,2] Regular user operation began in the fall of 2013.[3] In the future, the facility can possibly be upgraded by adding a second FEL covering the wavelength range from about 40 to 400 μm in the far-infrared (FIR) and Tera-Hertz (THz) regime. In this contribution we summarize the operational experience of the FHI FEL facility, which has opened up new possibilities for the ongoing research in gas phase spectroscopy, surface science, and physical chemistry at the FHI.

The IR radiation from the FHI FEL has, so far, been used for a variety of investigations including: (i) vibrational spectroscopy of clusters in the gas phase (including metal, metal-oxide, and water clusters); (ii) vibrational spectroscopy of molecules in the gas phase (including bio-molecules such as peptides and small proteins); (iii) molecular spectroscopy of ions embedded in superfluid helium nano-droplets at a temperature of 0.4 K; and (iv) second-harmonic generation in the Reststrahlen bands of solids such as cadmium telluride or silicon carbide.

Most molecular vibrational excitation energies lie in the so-called molecular fingerprint wavelength region from about 5 to 100 μm in the MIR. The fundamental vibrational modes in this regime can serve as a direct probe of molecular structure, which is why IR spectroscopy is one of the basic methods for molecular structure determination. Peptides and proteins, for instance, exhibit various excitations of the amidic molecular backbone. Examples are the C=O stretch mode (*Amide I*) around 1650 1/cm and N-H bending mode (*Amide II*) around

Further author information: (Send correspondence to W.S.)
W.S.: E-mail: wschoell@fhi-berlin.mpg.de

Advances in X-ray Free-Electron Lasers Instrumentation III, edited by Sandra G. Biedron
Proc. of SPIE Vol. 9512, 95121L · © 2015 SPIE · CCC code: 0277-786X/15/$18
doi: 10.1117/12.2182284

1500 1/cm. Furthermore, Reststrahlen bands of solids, stretching from the transverse optical (TO) to the longitudinal optical (LO) phonon frequencies, lie in the MIR wavelength region as well. For various solids of interest the Reststrahlen bands lie well within the scan range of the FHI FEL, e.g. from 800 to 1000 1/cm for silicon carbide and form 260 to 300 1/cm for gallium arsenide.

Tunable radiation for spectroscopy in the MIR region can, in principle, be generated by a number of sources. Especially Fourier Transform (FT) spectrometers allow for sub-wavenumber resolution in IR absorption experiments. However, for species that can only be produced in small quantities as well as for measurements that require a high temporal resolution FT-IR spectrometers have a limited applicability. Gas lasers, on the other hand, can deliver very high power levels at selected wavelength, but do not allow for continuous tuning. Tunable diode lasers are available over the entire MIR. However, in addition to their limited power of typically just a few mW, a single diode can usually only cover a spectral range of a few wavenumbers.

A different approach for generating tunable IR radiation is to frequency shift visible laser radiation into the IR using a nonlinear crystal such as, e.g., lithium niobate. This technique is particularly useful to generate pulsed IR radiation. In practice, intense pulses of tunable radiation can be generated down to about 10 μm. Beyond that, the obtainable pulse energy drops rapidly. For applications that rely on single photon excitation and that only require low intensity, sufficient light can, potentially, be generated down to about 20 μm. For still longer wavelengths, however, there is no good table-top radiation source available.

This is why measurements that need intense and continuously tunable radiation in the MIR, in many cases, can only be done with an IR FEL. The radiation from the FHI FEL comes in 5 to 10 μs long bursts (macro-pulses) containing thousands of micro-pulses. The length of the micro-pulses is on the order of 1 ps with a pulse-to-pulse separation of 1 ns. The micro-pulse energy is typically 5 to 10 μJ, corresponding to a macro-pulse energy of 50 to 100 mJ. The macro-pulse repetition frequency is typically set to 5 Hz.

This peculiar time structure of the FEL pulses is advantageous when lots of photons are needed on a time scale of tens of microseconds. For instance, multiple-photon excitation of dilute samples of molecules or clusters in the gas phase, in many cases, can only be realized by applying this kind of intense bursts from an IR FEL. For other studies, such as for instance time-resolved pump-probe experiments in the condensed phase, a pulse structure with a reduced micro-pulse repetition rate might be better suited. As described below, this additional mode of operation will also be available at the FHI FEL.

2. DESIGN OF THE FHI FEL

The FHI FEL has been described in detail before.[1,2,4–6] In brief, it includes two oscillator FELs; a MIR branch for wavelengths up to about 50 μm and a FIR branch for wavelengths from about 40 to 400 μm. The MIR FEL has been commissioned and is fully operational,[1,6] whereas the FIR FEL has been projected as a future facility upgrade. A normal-conducting linear accelerator provides electrons of up to 50 MeV energy with a beam transport system that feeds either of the two FEL branches or the electron diagnostics beamline as can be seen in Fig. 1. The beam transport line to the MIR undulator consists of two 90°-achromats. Another identical 90°-achromat has been prepared to deliver the beam to the FIR undulator. Downstream of the undulators 60°-dipole magnets transport the electron beam to beam dumps.

2.1 Electron accelerator

The accelerator system[2,7,8] was designed and built by Advanced Energy Systems, Inc. It combines a thermionic electron gun, a sub-harmonic buncher cavity, and two S-band (2.99 GHz) standing-wave $\pi/2$ copper linacs. The gridded electron gun is driven at the third sub-harmonic (1 GHz) producing a bunch length that is too long for efficient capture by the linac. Therefore, a 1 GHz buncher cavity is used to compress the bunch length. The first of the two linacs accelerates the electron bunches to a constant energy of 20 MeV. The second linac accelerates or decelerates the electrons to any final energy between 15 and 50 MeV. In addition, the electron bunch length can be compressed down to a minimum of 1 ps rms by a chicane between the linacs. The specifications of the accelerator system, listed in Tab. 1, include low longitudinal (< 50 keV psec) and transverse emittance ($< 20\,\pi$ mm mrad) at more than 200 pC bunch charge with a micro-bunch repetition rate of 1 GHz. The macro-bunch length and repetition rate are usually set to 10 or 12 μs and 5 Hz, respectively.

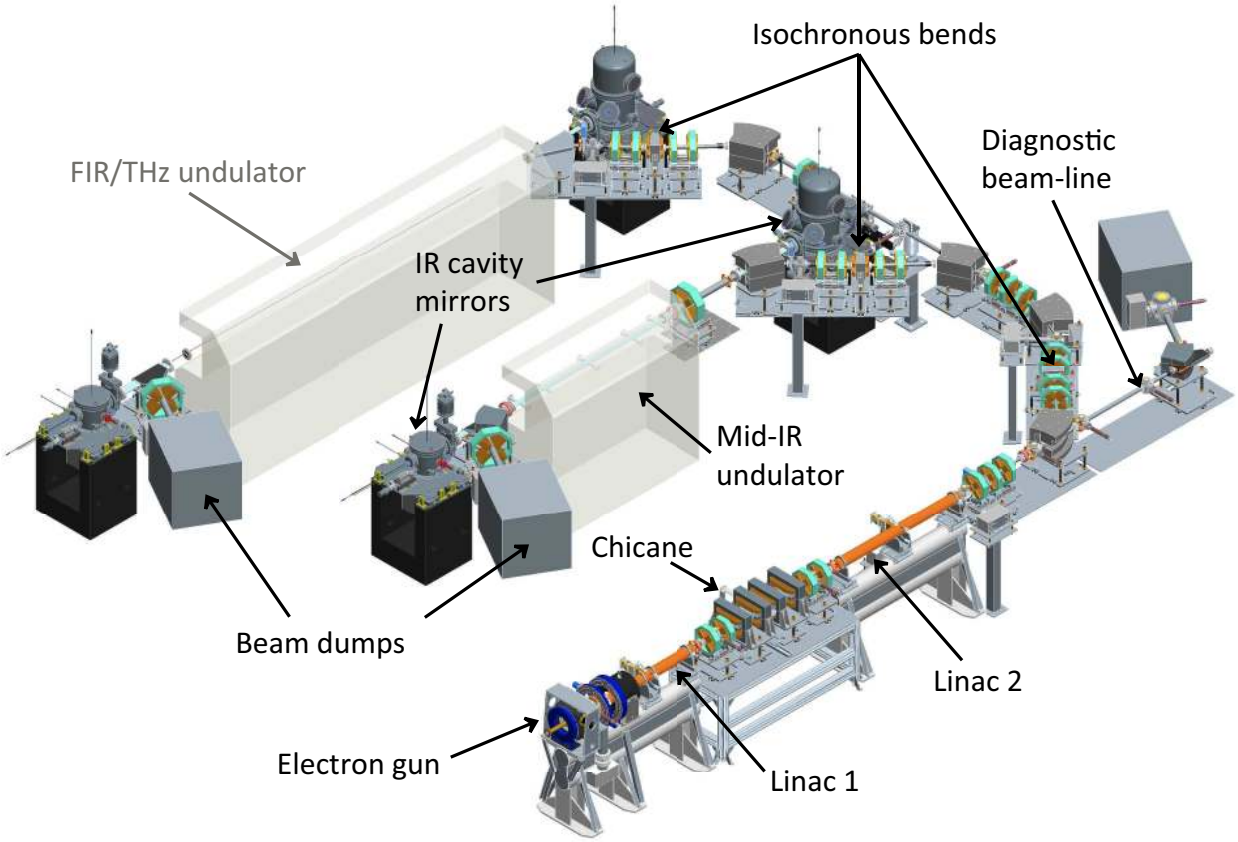

Figure 1. Overview of the FHI FEL installation showing the electron accelerator system, the MIR FEL (operational), and the FIR FEL (to be installed in the future).

A quadrupole triplet downstream of the second linac leads to the first dipole of the first 90°-achromat. The 90°-isochronous achromats are equipped with two 48°-dipoles and a small reverse 6°-dipole in between the four achromat quadrupoles. There is a quadrupole triplet in the straight section between the first and second 90° isochronous achromats which deliver the beam to the MIR undulator. The purpose of employing isochronous achromats is to maintain the temporal pulse profile and to minimize the effect of beam jitter on planned pump-probe experiments.

Table 1. Summary of electron beam parameters of the S-band linear accelerator. To best satisfy user demands the FEL is usually operated at one of 3 electron energies. At normal operation the micro-bunch length and the transverse emittance are not monitored.

Parameter	Unit	Specified	Typical
Electron energy	MeV	15 - 50	18, 26 or 36
Energy spread	keV	50	< 50
Energy drift per hour	%	0.1	< 0.1
Bunch charge	pC	200	220
Micro-bunch length	ps	1 - 5	–
Micro-bunch rep. rate	GHz	1	1
Macro-bunch length	μs	1 - 15	10 or 12
Macro-bunch rep. rate	Hz	≤ 20	5
Normalized rms transverse emittance	π mm mrad	20	–

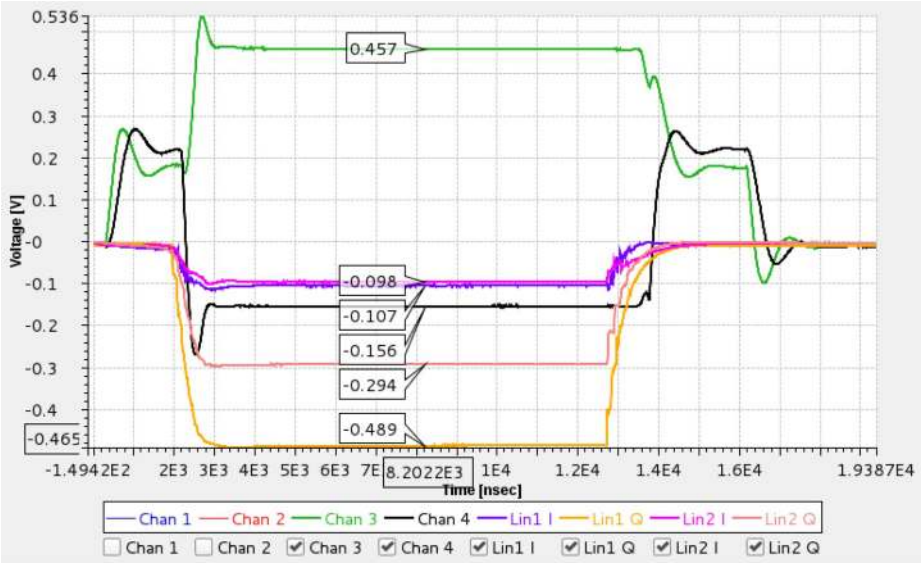

Figure 2. The I and Q components of the microwave fields in the sub-harmonic buncher cavity (green and black), 1st linac (violet and yellow), and 2nd linac (pink and mauve). Steady-state conditions are reached from 3 to 12.8 μs. The 1 GHz drive for the buncher field stops at 16.2 μs. The strong difference in the buncher field with (from 3 to 13 μs) and without electron beam loading (before 2 and after 15 μs) can be seen.

We have implemented a LLRF feed-forward system designed to help compensate for the cavity filling transients. The fields in the buncher and the linacs are sampled and demodulated giving I&Q signals that are fed into a digitizer for the controls to read and operate on. A typical screen shot of the I and Q traces is shown in Fig. 2 indicating flat behavior throughout the pulse. The same system can be used to provide a slow feed-back to reduce the long term drift of the electron energy. The feedback system, however, is usually not activated due to the fortunate fact that drifts of the accelerator system are close to negligible even over 12 hours shifts.

2.2 MIR FEL: undulator and cavity

In the MIR FEL a planar hybrid-magnet undulator is located within a 5.4 m long IR cavity. The undulator is 2 m long containing 50 periods of 40 mm (see Fig. 3). It is a wedged-pole design employing permanent magnets made out of a radiation resistent grade of NdFeB. It was designed and built by STI Optronics Inc. and has been described in detail before.[9] At a minimum gap of nominally 16.5 mm, a maximum root-mean-square undulator parameter K_{rms} of more than 1.6 is reached. This, in combination with the minimum electron energy of 15 MeV, corresponds to a theoretical maximum wavelength of more than 50 μm for the MIR system. In Tab. 2 we summarize the MIR undulator (operational) and the FIR undulator (planned).

The 5.4 m long MIR FEL cavity is formed by an end mirror and an out-coupling mirror. These are gold-plated copper mirrors of concave spherical shape with radius of curvature of 2.65 m and 3.51 m, respectively. The waist of the cavity mode is located at the undulator center which is shifted by 50 cm away from the cavity center. As hole-outcoupling is used, different hole diameters are needed for optimized performance at different wavelengths. To this end a motorized in-vacuum mirror changer is in use. It allows for precise positioning of any one out of five cavity mirrors with outcoupling-hole diameters of 0.75, 1.0, 1.5, 2.5, and 3.5 mm. It is part of the operational experience that the two outcoupling mirrors with 0.75 and 3.5 mm are hardly ever used, although they could help in optimizing the FEL performance at the shortest and the longest wavelengths. The other cavity mirror (end mirror) is mounted on a precision translation stage to allow for fine adjustment of the cavity length with 1 μm repeatability.

A commercial HeNe-laser interferometer (Agilent 10895A) has been implemented for feedback stabilization of the MIR cavity length. However, operational experience has shown that the feedback stabilization is not needed and, thus, hardly ever used. Slight drifts of the cavity length can occur on the time scale of many hours, but

Table 2. Summary of the most important parameters of the MIR FEL (commissioned) and FIR FEL (planned).

	MIR	FIR
Undulator		
Type	Planar hybrid	Planar hybrid or PPM
Material	NdFeB	NdFeB or SmCo
Period (mm)	40	110
No. of periods	50	40
Length (m)	2.0	4.4
Krms	0.5 - 1.6	1.0 - 3.0
IR-cavity		
Length (m)	5.4	7.2
Waveguide	none	1-D 10 mm high

are usually too small to disturb a user experiment. What has turned out to be highly useful is a wavelength synchronized cavity length adjustment. When activated it keeps the cavity at a length of $L_0 - q\lambda$, where L_0 is the nominal cavity length of 5.4 m, λ is the IR wavelength, q is a user defined factor (usually $0 < q < 5$), and $\Delta L = q\lambda$ is the cavity detuning. Keeping the cavity detuning at a constant multiple of λ during a wavelength scan significantly increases the wavelength range accessible by an undulator gap scan for a given electron energy. In addition, it helps to keep the relative bandwidth of the FEL line spectrum constant over the scan range as will be described below.

In addition to the standard 1 GHz micro-bunch repetition rate a reduced repetition-rate mode has been implemented. A repetition rate of 1 GHz corresponds to an electron bunch separation of 1 ns in time and, hence, 30 cm in space. As the MIR FEL cavity is 5.4 m long, this results in 36 equally spaced IR pulses circulating

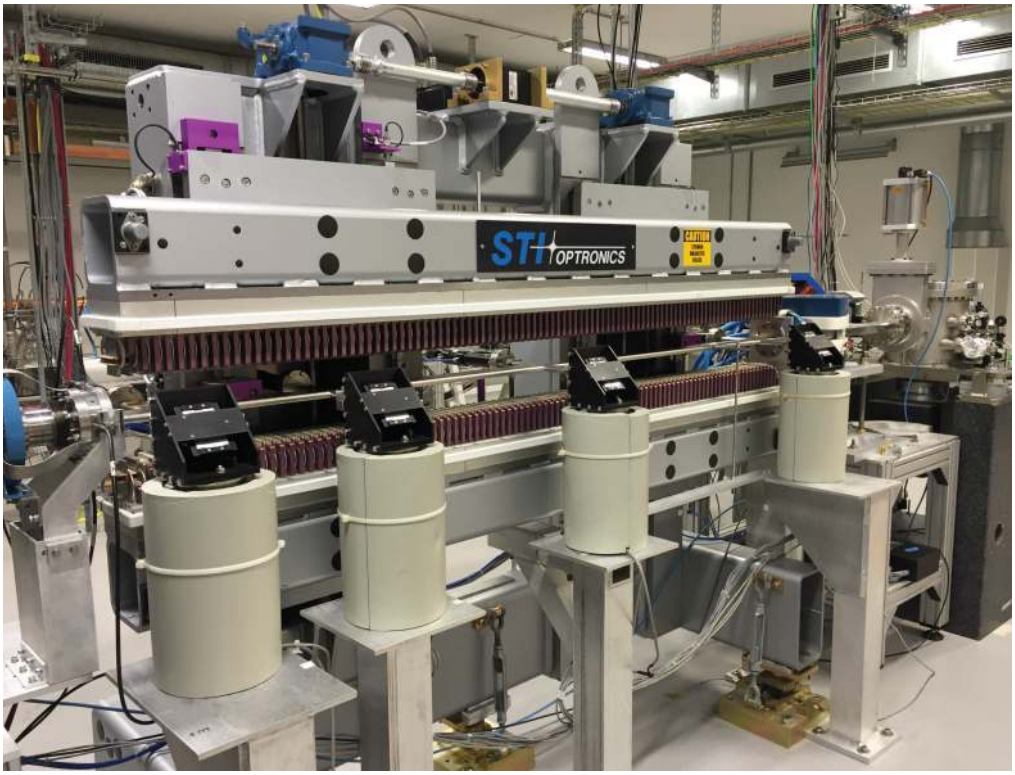

Figure 3. MIR FEL with undulator (center to left) and cavity end-mirror chambers (right) as of 2015.

Table 3. Reduced repetition rates of the electron micro-bunches needed to get different numbers of IR pulses simultaneously circulating the 5.4 m long MIR cavity.

Rep. rate (MHz)	1000	500	250	166.7	110.1	83.3	55.6	27.6
Number of pulses	36	18	9	6	4	3	2	1

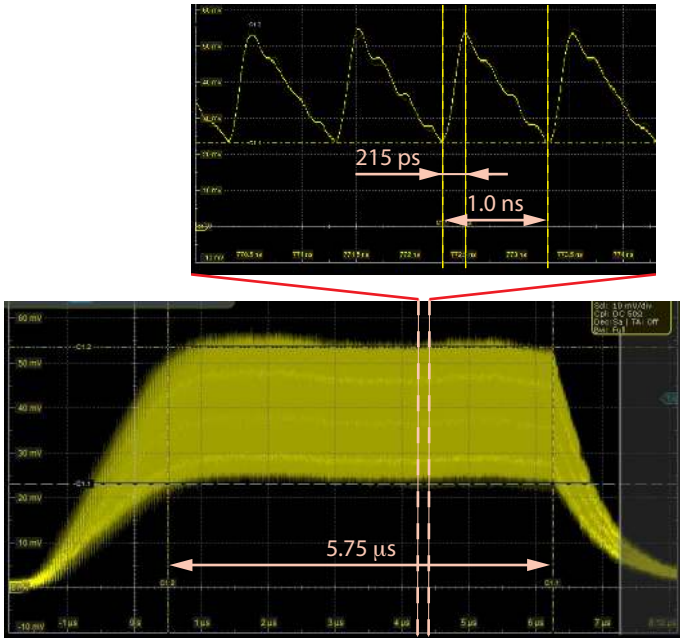

Figure 4. Detection of an FEL macro pulse at 6 μm wavelength with partial resolution of micro-pulses. The measurement was done using a fast detector from VIGO, model number PEM-10.6 in combination with a 4 GHz oscilloscope.

the cavity simultaneously. A single-pulse mode with just 1 IR pulse circulating the cavity can be achieved by reducing the electron-bunch repetition rate by a factor of 1/36 to 27.6 MHz. The other possible few-pulse modes together with the corresponding repetition rates are listed in Tab. 3.

To implement the reduced repetition rate modes listed in Tab. 3 one has to operate the gridded thermionic gun at the reduced pulse rate, while keeping the temporal profile of an individual electron bunch about the same as when running at 1 GHz. Therefore, voltage pulses which are not significantly longer then 500 ps with peak amplitude of about 150 to 200 V at the listed repetition rates need to be applied to the grid of the gun. To this end we can drive the grid with a custom-made grid pulser (Kentech Instruments Ltd.) which delivers electrical pulses with $>$ 160 V peak and full width at half maximum adjustable from 400 to 800 ps at repetition rates of 166.7, 110.1, 83.3, 55.6, or 27.6 MHz. This covers most of the repetition rates listed in Tab. 3.

3. CHARACTERIZATION OF THE MIR FEL RADIATION

The IR pulses coupled-out from the FEL cavity pass through a diamond window into the evacuated IR beamline and propagate a distance of 18 m from the FEL vault to the diagnostic station.[3] There, the spectrum of the IR radiation is measured by an in-vacuum Czerny-Turner grating spectrometer (Acton VM-504). A pyroelectric linear array detector with 128 elements and a total width of 1/2 inch (DIAS Infrared 128LT) is mounted to the spectrometer and allows for monitoring the FEL spectrum in-situ for each individual macro-pulse.

In addition, various commercial IR detectors are in use to determine the intensity of the FEL-pulses at different levels of sensitivity and temporal resolution. These include a 46 mm diameter, large area powermeter (Ophir PE50BB) used on a daily basis to determine macro-pulse energies. Several small area (4.5 mm x 4.5 mm) pyroelectric detectors (Eltec 420M7-0) combined with in-house made amplifiers are in use to monitor the

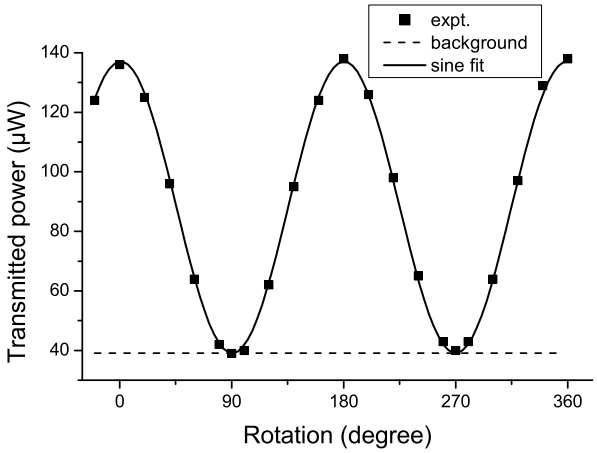

Figure 5. Determination of the polarization state of the FEL radiation. The FEL beam power was measured as a function of the angle of rotation of a commercial wire grid polarizer. The excellent fit of the data (after subtraction of the detector background signal) by a sine curve indicates linear polarization of the FEL beam. The FEL beam was strongly attenuated in these measurements to prevent damage to the polarizer.

temporal shape of the FEL macro-pulses. In addition, a sensitive liquid-nitrogen cooled mercury-cadmium-telluride (MCT) detector (Judson J15D24) is used for detection of low-intensity signals such as, for instance, higher harmonic signals (which can be generated within the FEL, but also by an external nonlinear crystal as will be shown below).

Furthermore, a very fast IR detector (VIGO PEM-10.6) with sub 250 ps time resolution and an active area of 2 mm x 2 mm is used to detect individual micro-pulses. Fig. 4 shows a measurement with this detector used in combination with a fast (4 GHz) oscilloscope without additional electrical amplification. At the standard micro-pulse repetition rate of 1 GHz individual micro-pulses are clearly resolved with a modulation depth of more than 50%. As can be seen in Fig. 4 this detector allows observing intensity changes on the single micro-pulse level.

The radiation from the FHI FEL is expected to be linearly polarized. Following from the design of the IR beamline,[3] with a total 8 mirrors between the FEL and the diagnostic station and another 6 mirrors from there to each user station, the polarization is expected to be horizontally linear at the user setup. Using a wire grid polarizer (Thorlabs WP50H-K; micro-fabricated aluminum wires on a KRS-5 substrate with 34 mm clear aperture) we determined the polarization state of the FEL radiation at one of the user stations. The transmitted power as a function of the polarizer rotation angle is shown in Fig. 5. The results indicate a horizontally linear polarization of the FEL radiation.

3.1 Temporal characterization of the FEL micro-pulses by autocorrelation measurements

Even for the fast IR detector (Fig. 4) the time resolution is by far insufficient to reveal the length and shape of the individual ps-long micro-pulses. For this reason we have installed an autocorrelation setup, shown schematically in Fig. 6A, to characterize the micro-pulse shape.[10] FEL pulses are split by a 50:50 ZnSe beam splitter (Edmund Optics). The length of one of the beam paths can be varied by a precision motorized translation stage to adjust the relative temporal delay between the two partial beams. Both beams are separately focused by 6" focal-length mirrors onto the same spot on a CdTe crystal (MaTeck GmbH) with an angle of $\approx 30^\circ$ between the beams.

At temporal overlap of the pulses from both paths, nonlinear effects in the CdTe crystal lead to the generation of second harmonic (SH) radiation which is emitted in the direction exactly in between the reflected fundamental beams as indicated in Fig. 6A. After spatial filtering to block the fundamental beams, the SH signal is detected with a liquid-nitrogen cooled MCT detector.

In Fig. 6B we show a series of SH autocorrelation measurements for various cavity-length detunings ΔL ranging from -2 to -50 μm. Each curve shows the SH signal as a function of the delay between the two beam

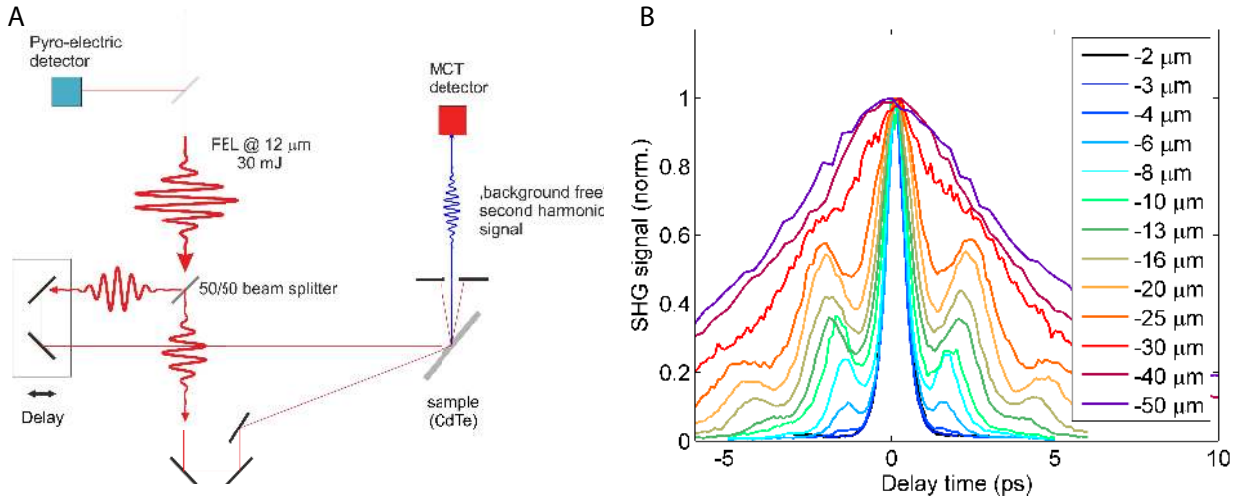

Figure 6. Autocorrelation measurements. A schematic of the autocorrelation setup is shown in (A). In (B) the second harmonic signal is plotted as a function of the path length difference for various cavity detunings. In these measurements at a wavelength of 12 μm the electron macro-bunch length was set to 6 μs leading to 1-4 μs long optical macro-pulses depending on the actual gain for a given detuning ΔL. The absolute values of ΔL might be shifted since the absolute cavity length corresponding to $\Delta L = 0$ is not exactly known and can only be estimated.

paths. For the smallest ΔL of just a few micron we find narrow, single-peaked curves. The full width at half maximum (FWHM) of about 600 fs of the SH autocorrelation curve for $\Delta L = -2$ μm corresponds to a micro-pulse FWHM of 420 fs, thereby indicating the potential of the FEL to generate ultrashort IR pulses. With increasing magnitude of ΔL the central peak width increases and additional side peaks appear on both sides of the central peak at a separation increasing from ± 1.5 to ± 2.5 ps when ΔL is changed from -4 to -25 μm. For even larger magnitudes of ΔL the central and side peaks smear out forming a single broad peak with a FWHM of 8 ps at $\Delta L = -50$ μm.

All these features are in good agreement with the expected behavior of an oscillator FEL as it was observed previously at the FELIX IR FEL.[11–14] An oscillator FEL can operate in different regimes depending on the cavity detuning ΔL. At $\Delta L = 0$ the gain drops to zero and no lasing is achieved. Shortening the optical cavity leads to an increase in gain and a simultaneous decrease in saturation intensity. For small detuning, $0 > \Delta L \geq -3\lambda$, the micro-pulses are composed of multiple equally-spaced sub-pulses, just as the ones seen in Fig. 6B. This is the regime of limit-cycle oscillations, where the FEL power exhibits oscillations over the duration of the macro-pulse.[11,13] This phenomenon relates to reduced optical group velocity of the cavity mode before saturation is reached, followed by recovery of group velocity upon saturation, causing the optical pulse to lose temporal overlap with the electron bunch and formation of a second (third, etc.) sub-pulse. For larger detuning, the laser operates in the so-called stable focus limit,[13] in which single, highly asymmetric and relatively long pulses are emitted.[14]

4. SELECTED FHI FEL USER EXPERIMENTS: ACTION SPECTROSCOPY

Common to almost all spectroscopic experiments at the FHI FEL is the fact that, unlike in classical absorption spectroscopy, a spectrum is not recorded by measuring the reduction of the transmitted IR intensity as a function of wavelength. Especially for gas phase samples the absorption signal would be too small to yield a decent signal-to-noise ratio. To circumvent this problem *action spectroscopy* is used: Some action (actually "reaction") of the molecules or clusters, triggered by absorption of one or many FEL photons, is detected and recorded. The action can be, for instance, molecular fragmentation or detachment of a weakly attached tagging molecule (with the change in mass detected by mass spectrometry); it can be ejection of a molecule from a helium nano-droplet; or it can be a change of magnetic or optical properties of a solid sample following excitation by the FEL radiation. In the following we describe FHI FEL user experiments employing action spectroscopy.

4.1 Neutral and charged clusters in the gas phase

4.1.1 Strongly bound clusters

The IR FEL radiation is used by the group of André Fielicke (FHI and TU Berlin) to investigate structure and chemistry of strongly bound clusters in the gas phase. In their molecular-beam apparatus the group has the capabilities to study neutral as well as charged species. The clusters are produced using either a single-target or a dual-target laser ablation source allowing the generation of pure or alloy clusters of controlled compositions, respectively. Complexes of the clusters with ad-molecules such as CO, O_2, H_2O can be formed and IR spectroscopy is used to characterize the bonding of these species to the clusters.

Systems studied with the FHI FEL, so far, include carbon monoxide bound to transition metal clusters and co-adsorbates of oxygen and water on small gold clusters. Further studies focused on neutral silicon clusters doped by boron or nitrogen atoms. For CO bound to cobalt-manganese clusters, for instance, it was found that the CO vibrational frequency is shifted to lower frequency with increasing manganese content. These studies allow probing the effects of alloying on the d-band center that controls the strength of the π-backbonding to the CO.

4.1.2 Ionic metal oxide and water clusters in the gas phase

Further studies of gas-phase clusters have been done in collaboration with the group of Knut Asmis (FHI and University of Leipzig). Charged aluminum oxide and iron oxide clusters, prepared in an ion trap, cooled down to temperatures on the order of 20 K, and tagged with one or a few deuterium molecules or helium atoms are excited by the FHI FEL radiation. Vibrational excitation of the metal oxide cluster leads to detachment of the relatively weakly bound D_2 or He tag. Thus, vibrational spectra of the clusters can be acquired by observing the cluster-tag dissociation rate with a mass spectrometer as a function of IR wavelength. Comparison of the observed IR spectra with theoretical ones calculated for various cluster geometries permits uncovering of the metal-oxide cluster structures.

Furthermore, the Asmis group also applied the MIR radiation from the FHI FEL to investigate the structural properties of the water clusters $H_3O^+(H_2O)_{20}$ and $Cs^+(H_2O)_{20}$,[15] which are referred to as *magic* clusters because of their enhanced stability. In addition, the Asmis group discovered what is called a bidentate binding motif in the structure of the anionic magnesium-CO_2 complex $[ClMgCO_2]^-$.[16]

4.2 Spectroscopy of bio-molecules

4.2.1 IR spectroscopy combined with ion mobility spectrometry

In an experiment performed by the user group of one of the authors (GvH) the FEL has been used to reveal information about the structure of bio-molecules in the gas phase. To this end the group combines the method of ion mobility spectrometry with IR spectroscopy. In the ion mobility setup the molecules in the gas phase are not only mass-to-charge selected but also isomer and conformer selected by exploiting different arrival times in a drift cell filled with several mbar of helium or nitrogen gas.

As an example in Fig. 7 we show IR spectra of two forms of the protonated benzocaine molecule, which were separated according to their different drift arrival times in the ion mobility spectrometer.[17] For each of the forms an IR photo-fragmentation spectrum is gained separately by recording the depletion of the mass spectrometer signal as a function of FEL wavelength. As can be seen in Fig. 7B significantly different spectra are found for the two forms. By comparison with calculated spectra the molecular forms can be identified with two protomers of distinct localization of the added proton. Benzocaine finds widespread use as a local anesthetics. An improved understanding of the molecular structure and its dependence on ambient conditions can, potentially, contribute clarifying the details of the way the anesthetics works.

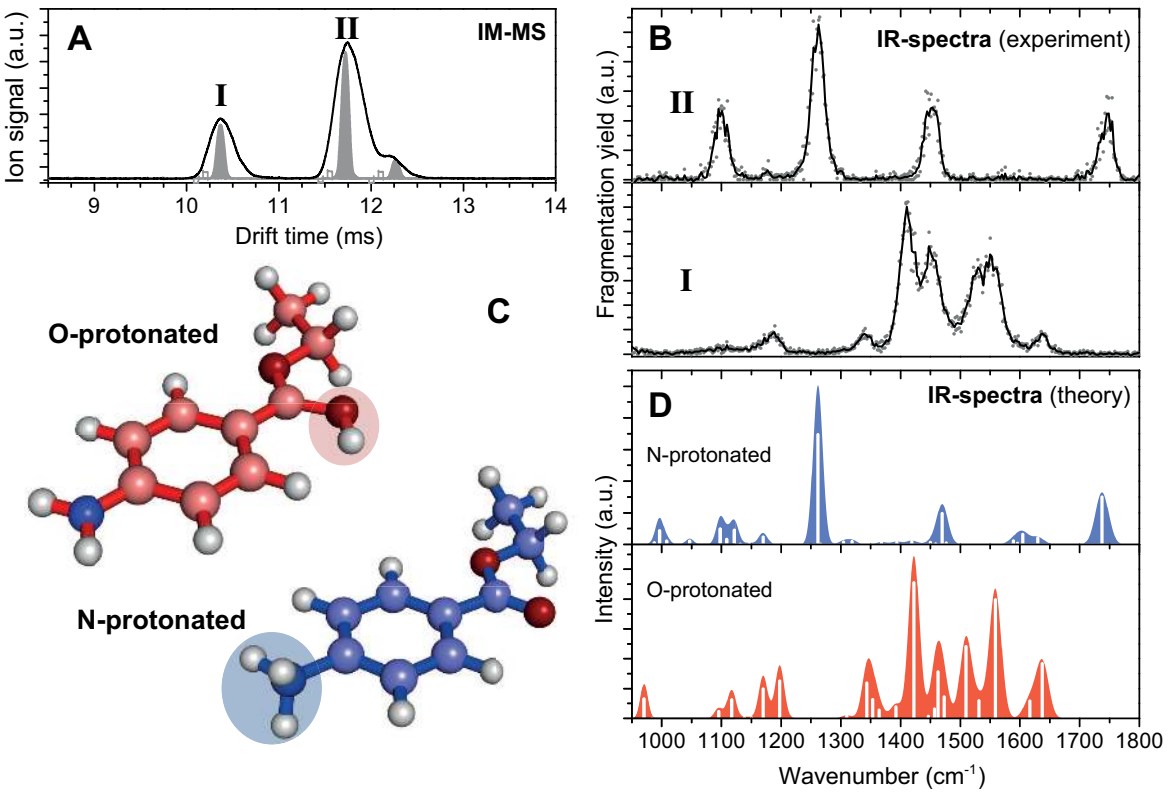

Figure 7. IR spectra of protonated benzocaine in the gas phase obtained by combining ion-mobility mass spectrometry (IM MS) with IR spectroscopy. Two different forms (labeled I and II) of the molecule are found and separated by their different drift times (A). For each form an IR photo-fragmentation spectrum is recorded (B). By comparison with calculated spectra (D) they can be assigned to the two protomers shown in (C) which differ by the location of the attached proton. This figure is a modified copy from Ref.[17]

4.2.2 Spectroscopy of charged peptides and small proteins embedded in superfluid helium nano-droplets

For the last decade helium nano-droplet isolation spectroscopy has been used in many labs to record optical spectra of molecules at ultracold conditions.[18] Molecules embedded to superfluid helium nano-droplets are cooled to the droplet temperature of 0.4 K. Due to the weak interaction between the superfluid helium and the dopant molecule, the droplet causes only little perturbation to the optical spectra. In addition, helium is optically transparent over the entire optical range.

In most previous experiments, the chromophore molecules were brought into the gas phase via thermal evaporation and then picked up by the droplets. That approach does not work for samples that can not be evaporated (like bio-molecules). At the FHI an apparatus has been setup where bio-molecules are brought into the gas phase by electrospray ionization, mass-to-charge selected in a mass spectrometer and, subsequently, stored in an ion trap. The helium droplets traverse the trap and pick up the ions. IR spectra of the mass-to-charge selected ions embedded in helium droplets can then be recorded.

As an example, in Fig. 8 we show IR spectra of the protonated penta-peptide leucine-enkephalin (LEK). The lines observed are much narrower than those measured when using conventional gas-phase methods. We present a comparison of the spectra of the monomer and the dimer in Fig. 8. The dimer spectrum contains fewer peaks than the monomer spectrum. This indicates a uniform structure of the protonated LEK dimers embedded in He droplets. A detailed quantitative analysis of the spectra is expected to reveal insight into the structural properties of the small peptides and the bonds they form.

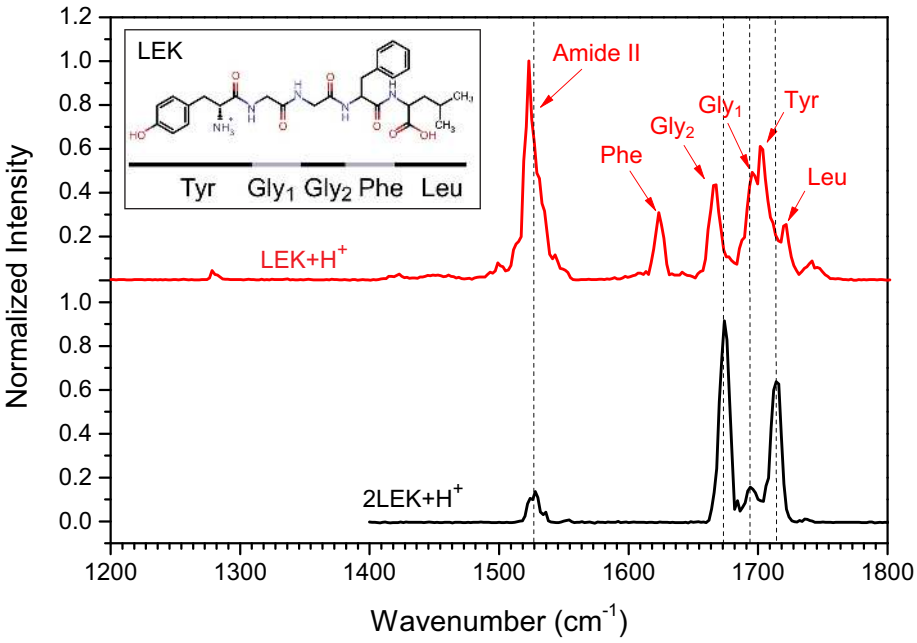

Figure 8. IR spectrum of the penta-peptide leucine enkephalin (LEK) embedded in a superfluid helium nano-droplet at a temperature of 0.4 K. LEK is a penta-peptide composed of the amino acids tyrosine (Tyr), glycine (Gly), phenylalanine (Phe), leucine (Leu) as depicted in the inset. Comparison of the protonated monomer (LEK+1H, red trace) with the protonated dimer (2LEK+1H, black trace) reveals fewer peaks for the dimer. The peaks of the monomer have been assigned to individual amino acids within the peptide as indicated.

4.3 Nonlinear IR spectroscopy of solid state systems

MIR radiation from the FHI FEL has also been used to investigate solid state systems. The user group of one of the authors (AP) has applied FEL pulses to generate second harmonic radiation in nonlinear optical crystals like CdTe and GaSe. The second harmonic signal has been exploited in autocorrelation experiments, described in Section 3.1 above, to characterize the FEL micro-pulse temporal shape. Further investigations of solid state systems include ultrafast, time-resolved experiments. In these studies the FEL pulses serve as short pump pulses. Various probes, such as visible reflectivity or sample magnetization, can be used to investigate fundamental interactions among low-energy excitations. Within this project it is also planned to synchronize the FEL micro-pulses with femtosecond pulses from a near-IR table-top laser within sub-ps accuracy.

5. ACKNOWLEDGMENTS

We thank Christian Schewe for help with the measurements. We further thank Ulf Lehnert, Peter Michel, Wolfgang Seidel, Rudi Wünsch (FELBE at Helmholtz-Zentrum Dresden-Rossendorf, Germany); Lex van der Meer (FELIX at Radboud University Nijmegen, The Netherlands); Johannes Bahrdt, Andreas Gaupp, Klaus Ott, and Ernst Weihreter (BESSY II at Helmholtz-Zentrum Berlin, Germany); Jangho Park and John Rathke (Advanced Energy Systems Inc., Medford, NY, USA); Dave Dowell, Kevin Jordan, Ralph Lange, Henrik Loos, and Lloyd Young (consultants to Advanced Energy Systems Inc., Medford, NY, USA); Steven Gottschalk (STI Optronics Inc., Bellevue, WA, USA); Wolfgang Erlebach, Georg Heyne, Andreas Liedke, Gerard Meijer, Viktor Platschkowski, Patrik Schlecht, Mike Wesemann, and Weiqing Zhang (FHI Berlin, Germany) for their valuable contributions to design, construction, and commissioning of the FHI FEL. We also thank Doo-Sik Ahn, Knut Asmis, Tim Esser, Matias Fagiani, André Fielicke, Ana Isabel Gonzalez Florez, Harald Knorke, Jongcheol Seo, Xiaowei Song, and Stephan Warnke for fruitful discussions about the user experiments discussed in this work.

REFERENCES

[1] Schöllkopf, W., Gewinner, S., Erlebach, W., Heyne, G., Junkes, H., Liedke, A., Platschkowski, V., Helden, G. v., Zhang, W., Meijer, G., Bluem, H., Davidsaver, M., Dowell, D., Jordan, K., Lange, R., Loos, H., Park, J., Rathke, J., Todd, A. M. M., Young, L. M., Lehnert, U., Michel, P., Seidel, W., Wünsch, R., and Gottschalk, S. C., "First Lasing of the IR FEL at the Fritz-Haber-Institut Berlin," in [*Proceedings of FEL 2012, Nara, Japan*], (MOOB01), 1 – 4 (2013).

[2] Bluem, H. P., Dowell, D., Loos, H., Park, J., Todd, A. M. M., Young, L. M., Gewinner, S., and Schöllkopf, W., "Accelerator Beamline Performance for the IR FEL at the Fritz-Haber-Institut, Berlin," in [*Proceedings of FEL 2012, Nara, Japan*], (WEOC04), 365 – 368 (2013).

[3] Schöllkopf, W., Gewinner, S., Erlebach, W., Junkes, H., Liedke, A., Meijer, G., Paarmann, A., Helden, G. v., Bluem, H., Dowell, D., Lange, R., Rathke, J., Todd, A. M. M., Young, L. M., Lehnert, U., Michel, P., Seidel, W., Wünsch, R., and Gottschalk, S. C., "The new IR FEL facility at the Fritz-Haber-Institut in Berlin," in [*Proceedings of FEL 2014, Basel, Switzerland*], (WEB04), 629 – 634 (2014).

[4] Bluem, H., Christina, V., Dalesio, B., Douglas, D., Dowell, D., Jordan, K., Park, J. H., Rathke, J., Todd, A. M. M., Young, L. M., Gewinner, S., Junkes, H., Meijer, G., Schöllkopf, W., Helden, G. v., Zhang, W., Lehnert, U., Michel, P., Seidel, W., Wünsch, R., Gottschalk, S., and Kelly, R., "The Fritz Haber Institute THz FEL Status," in [*Proceedings of FEL 2010, Malmo, Sweden*], (MOPA09), 45 – 47 (2010).

[5] Schöllkopf, W., Gewinner, S., Erlebach, W., Junkes, H., Liedke, A., Helden, G. v., Zhang, W., Meijer, G., Bluem, H., Christina, V., Cole, M. D., Ditta, J., Dowell, D., Jordan, K., Lange, R., Park, J. H., Rathke, J., Schultheiss, T., Todd, A. M. M., Young, L. M., Lehnert, U., Michel, P., Seidel, W., Wünsch, R., and Gottschalk, S. C., "Status of the Fritz Haber Institute THz FEL," in [*Proceedings of FEL 2011, Shanghai, China*], (TUPB30), 315 – 317 (2012).

[6] Schöllkopf, W., Gewinner, S., Erlebach, W., Heyne, G., Junkes, H., Liedke, A., Meijer, G., Platschkowski, V., Helden, G. v., Bluem, H., Davidsaver, M. A., Dowell, D., Jordan, K., Lange, R., Loos, H., Rathke, J., Todd, A. M. M., Young, L. M., Lehnert, U., Michel, P., Seidel, W., Wünsch, R., and Gottschalk, S. C., "The IR and THz Free-Electron Laser at the Fritz-Haber-Institut," in [*Proceedings of FEL 2013, New York, NY, USA*], (WEPSO62), 657 – 660 (2013).

[7] Todd, A. M. M., Bluem, H., Christina, V., Cole, M. D., Ditta, J., Dowell, D., Jordan, K., Lange, R., Park, J. H., Rathke, J., Schultheiss, T., Young, L. M., Schöllkopf, W., Gewinner, S., Erlebach, W., Junkes, H., Liedke, A., Helden, G. v., Zhang, W., Meijer, G., and Gottschalk, S. C., "Commissioning Status of the Fritz Haber Institute THz FEL," in [*Proceedings of IPAC2011, San Sebastián, Spain*], (THPC106), 3137 – 3139 (2011).

[8] Todd, A. M. M., Bluem, H., Ditta, J., Dowell, D., Jordan, K., Lange, R., Loos, H., Park, J. H., Rathke, J., Young, L. M., Erlebach, W., Gewinner, S., Helden, G. v., Junkes, H., Liedke, A., Meijer, G., Schöllkopf, W., Zhang, W., Lehnert, U., Michel, P., Seidel, W., Wünsch, R., and Gottschalk, S. C., "Commissioning of the Fritz Haber Institute Mid-IR FEL," in [*Proceedings of IPAC 2012, New Orleans, Louisiana, USA*], (TUPPP087), 1792 – 1794 (2012).

[9] Gottschalk, S. C., DeHart, T. E., Kelly, R. N., Offenbacker, M. A., Valla, A. S., Bluem, H., Dowell, D., Rathke, J., Todd, A. M. M., Gewinner, S., Junkes, H., Meijer, G., Schöllkopf, W., Zhang, W., and Lehnert, U., "Design and Performance of the Wedged Pole Hybrid Undulator for the Fritz-Haber-Institut IR FEL," in [*Proceedings of FEL 2012, Nara, Japan*], (THPD13), 575 – 578 (2013).

[10] Xu, J., Knippels, G. M. H., Oepts, D., and van der Meer, A. F. G., "A far-infrared broadband $(8.5-37\mu\mathrm{m})$ autocorrelator with sub-picosecond time resolution based on cadmium telluride," *Opt. Commun.* **197**, 379 (2001).

[11] Jaroszynski, D. A., Bakker, R. J., van der Meer, A. F. G., Oepts, D., and van Amersfoort, P. W., "Experimental observation of limit-cycle oscillations in a short-pulse free-electron laser," *Phys. Rev. Lett.* **70**, 3412 (1993).

[12] Bakker, R. J., Jaroszynski, D. A., van der Meer, A. F. G., Oepts, D., and van Amersfoort, P. W., "Short-pulse effects in a free-electron laser," *IEEE J. Quantum Electron.* **30**, 1635 (1994).

[13] Knippels, G. M. H., van der Meer, A. F. G., Mols, R. F. X. A. M., Oepts, D., and van Amersfoort, P. W., "Formation of multiple subpulses in a free-electron laser operating in the limit-cycle mode," *Phys. Rev. E* **53**, 2778 (1996).

[14] MacLeod, A. M., Yan, X., Gillespie, W. A., Knippels, G. M. H., Oepts, D., van der Meer, A. F. G., Rella, C. W., Smith, T. I., and Schwettman, H. A., "Formation of low time-bandwidth product, single-sided exponential optical pulses in free-electron laser oscillators," *Phys. Rev. E* **62**, 4216 (2000).

[15] Fournier, J. A., Wolke, C. T., Johnson, C. J., Johnson, M. A., Heine, N., Gewinner, S., Schöllkopf, W., Esser, T. K., Fagiani, M. R., Knorke, H., and Asmis, K. R., "Site-specific spectral signatures of water molecules in the "magic" $H_3O^+(H_2O)_{20}$ and $Cs^+(H_2O)_{20}$ clusters in the regions of the OH(D) stretches and low frequency librations (215-1000 cm^{-1})," *PNAS* **111**, 181327 (2014).

[16] Miller, G. B. S., Esser, T. K., Knorke, H., Gewinner, S., Schöllkopf, W., Heine, N., Asmis, K. R., and Uggerud, E., "Spectroscopic Identification of a Bidentate Binding Motif in the Anionic Magnesium-CO_2 Complex $[ClMgCO_2]^-$," *Angew. Chem. Int. Ed.* **53**, 14407–10 (2014).

[17] Warnke, S., Seo, J., Boschmans, J., Sobott, F., Scrivens, J. H., Bleiholder, C., Bowers, M. T., Gewinner, S., Schöllkopf, W., Pagel, K., and von Helden, G., "Protomers of Benzocaine: Solvent and Permittivity Dependence," *J. Am. Chem. Soc.* **137**, 4236 (2015).

[18] Vilesov, A. F. and Toennies, J. P., "Superfluid helium droplets: A uniquely cold nanomatrix for molecules and molecular complexes," *Angew. Chem. Int. Ed.* **43**, 2622–2648 (2004).